Plant Physiology, January 2000, Vol. 122, pp. 157–167, www.plantphysiol.org © 2000 American Society of Plant Physiologists

Calmodulin Activation of an Endoplasmic Reticulum-Located Calcium Pump Involves an Interaction with the N-Terminal Autoinhibitory Domain[1]

Ildoo Hwang, Jeffrey F. Harper, Feng Liang[2], and Heven Sze*

Department of Cell Biology and Molecular Genetics, and Maryland Agricultural Experiment Station, University of Maryland, College Park, Maryland 20742 (I.H., F.L., H.S.); and Department of Cell Biology, The Scripps Research Institute, La Jolla, California 92037 (J.F.H.)

To investigate how calmodulin regulates a unique subfamily of Ca^{2+} pumps found in plants, we examined the kinetic properties of isoform *ACA2* identified in Arabidopsis. A recombinant ACA2 was expressed in a yeast K616 mutant deficient in two endogenous Ca^{2+} pumps. Orthovanadate-sensitive $^{45}Ca^{2+}$ transport into vesicles isolated from transformants demonstrated that ACA2 is a Ca^{2+} pump. Ca^{2+} pumping by the full-length protein (ACA2-1) was 4- to 10-fold lower than that of the N-terminal truncated ACA2-2 (Δ2–80), indicating that the N-terminal domain normally acts to inhibit the pump. An inhibitory sequence (IC_{50} = 4 μM) was localized to a region within valine-20 to leucine-44, because a peptide corresponding to this sequence lowered the V_{max} and increased the K_m for Ca^{2+} of the constitutively active ACA2-2 to values comparable to the full-length pump. The peptide also blocked the activity (IC_{50} = 7 μM) of a Ca^{2+} pump (AtECA1) belonging to a second family of Ca^{2+} pumps. This inhibitory sequence appears to overlap with a calmodulin-binding site in ACA2, previously mapped between asparatate-19 and arginine-36 (J.F. Harper, B. Hong, I. Hwang, H.Q. Guo, R. Stoddard, J.F. Huang, M.G. Palmgren, H. Sze [1998] J Biol Chem 273: 1099–1106). These results support a model in which the pump is kept "unactivated" by an intramolecular interaction between an autoinhibitory sequence located between residues 20 and 44 and a site in the Ca^{2+} pump core that is highly conserved between different Ca^{2+} pump families. Results further support a model in which activation occurs as a result of Ca^{2+}-induced binding of calmodulin to a site overlapping or immediately adjacent to the autoinhibitory sequence.

The importance of Ca^{2+} in signaling, growth, and development has long been recognized; however, the temporal and spatial regulation of Ca^{2+} levels in plant cells is poorly understood (Bush, 1995; Sanders et al., 1999). A variety of signals, such as drought and salinity, cause transient opening of Ca^{2+} channels in the plasma membrane (PM) and/or endomembranes. A current model is that [Ca^{2+}] fluctuations in microdomains of the cytosol are sensed and decoded to produce specific cellular and physiological responses (Sanders et al., 1999), such as in abscisic acid-induced closure of stomatal aperture (Ward et al., 1995). The frequency and pattern of cytosolic Ca^{2+} transients are determined by the coordinate regulation of two opposing fluxes: Ca^{2+} influx via channels and Ca^{2+} efflux via active transporters. Ca^{2+}-pumping ATPases comprise the bulk of the active transporters, and serve three major functions: (a) to lower cytosolic Ca^{2+}; (b) to replenish Ca^{2+} sinks in the vacuole and endoplasmic reticulum (ER); and (c) to supply Ca^{2+} in endoluminal compartments for biochemical functions (Sanders et al., 1999).

In spite of the significant functions, little is known at the molecular level about the different Ca^{2+} pumps or their specific modes of regulation. Both biochemical and molecular studies provide evidence for two distinct families of Ca^{2+} pumps in plants often referred to as "ER-type" (or type IIA) and "PM-type" (or type IIB) (Geisler et al., 1999). ER-type Ca^{2+} pumps, like the Arabidopsis ECA1, are often localized on the ER, and are insensitive to calmodulin (Liang et al., 1997; Liang and Sze, 1998). PM-type Ca^{2+} pumps, however, are stimulated by calmodulin (Hwang et al., 1997).

Although calmodulin-stimulated Ca^{2+} pumps from plants are more closely related to animal plasma membrane Ca^{2+}-ATPases in protein sequence, this type of pump in plants is localized on the vacuolar membrane (Askerlund, 1996, 1997; Malmstrom et al., 1997), the ER (Hwang et al., 1997; Hong et al., 1999), and the plasma membrane (Rasi-Caldogno et al., 1992). At least two different Ca^{2+} pumps from plants had been purified by calmodulin-affinity chromatography. One protein of 111 kD was localized to the vacuole of cauliflower (Askerlund, 1996, 1997) and another protein of 133 kD (Bonza et al., 1998) from the PM of radish. Several plant genes encoding homologs of animal PM Ca^{2+} pumps have been isolated, including ACA1/PEA (Huang et al., 1993), ACA2 (Harper et al., 1998), and BCA1. Evidence indicates that BCA1 encodes a calmodulin-stimulated Ca^{2+} pump based on correspondence to peptide sequences from a purified vacuolar pump (Malmstrom et al., 1997).

[1] This work was supported in part by the Department of Energy (grant no. DE–FG02–95ER20200 to H.S. and grant no. DE–FG03–94ER20152 to J.F.H.), and a joint grant from the National Aeronautics and Space Administration and National Science Foundation (grant no. IBN–9416038) for the Plant Sensory Systems Collaborative Research Network.

[2] Present address: Department of Bioinformatics, The Institute for Genomic Research, 9712 Medical Center Drive, Rockville, MD 20850.

* Corresponding author; e-mail hs29@umail.umd.edu; fax 301–314–9082.

An intriguing discovery about plant plasma membrane Ca^{2+}-ATPase homologs is that BCA1 and ACA2 possess a regulatory domain at the N terminus instead of the C terminus (Malmstrom et al., 1997; Harper et al., 1998). We previously showed that the full-length ACA2 failed to restore growth on Ca^{2+}-depleted medium of a yeast mutant harboring a disruption of its endogenous Ca^{2+} pumps. However, a truncated ACA2 (Δ2–80 residues) rescued the mutant phenotype and displayed constitutively active Ca^{2+}-dependent ATPase activity (Harper et al., 1998). These results suggested that *ACA2* encodes a Ca^{2+} pump.

In the present study we show that ACA2 can transport Ca^{2+}, providing the first direct evidence (to our knowledge) that ACA2 is a Ca^{2+} pump. Furthermore, we determine the kinetic properties to identify the autoinhibitory sequence and to understand how the pump is regulated by calmodulin. The velocity of the full-length protein and its affinity for Ca^{2+} were increased by calmodulin to values equivalent to those observed for the de-regulated (N-terminally truncated) mutant in the absence of calmodulin. We also show that a peptide sequence derived from the N-terminal domain can inhibit the activity of the de-regulated pump. Our results support a model in which activation occurs as a result of calmodulin binding to a site overlapping or immediately adjacent to an autoinhibitory sequence located in the N-terminal domain, and thereby displacing its inhibitory interactions.

MATERIALS AND METHODS

Yeast Strains and Their Growth Media

Saccharomyces cerevisiae strains W303-1A (*MATa*, *leu2*, *his3*, *ade2*, *trp1*, and *ura3*) and K616 (*MATa pmr1::HIS3 pmc1::TRP1 cnb1::LEU2, ura3*) were used (Cunningham and Fink, 1994). Wild-type W303-1A and mutant *K616* strains were grown for 24 h in standard yeast peptone dextrose medium before transformation. *K616* strain grows better in media supplemented with 10 mM $CaCl_2$. After transformation with pYX plasmid constructs, transformants were selected on synthetic complete medium minus uracil (SC-URA). The medium consisted of 1 mM Ca^{2+}, 6.7 g/L yeast nitrogen base without amino acids, 2 g/L drop-out mix without uracil, and 2% (v/v) Glc as a carbon source (Rose et al., 1990).

cDNA and Constructs

Contructs used for the expression of a full-length ACA2 and truncated ACA2-2 (ΔP80) were previously described, pYX-ACA2-1 and pYX-ACA2-2, respectively (Harper et al., 1998). The vector used was pYX-112 (formerly distributed by Novagen, Madison, WI). ACA2 and ACA2-2 were expressed under the control of a strong constitutive promoter from triose phosphate isomerase. The pYX-112 vector contains URA3 as a selection marker.

Yeast Transformation and Growth

Wild-type and mutant strains of *S. cerevisiae* were transformed with pYX vector alone, pYX-ACA2-1, or pYX-ACA2-2 by the LiOAc/polyethylene glycol methods (Becker and Guarente, 1991) and selected for uracil prototrophy by plating on SC-URA medium. The Ura^+ colonies were picked and grown for 2 to 3 d on SC-URA agar plates.

To measure growth, K616 transformants were grown overnight and the culture was suspended in 50 mL of SC-URA medium at pH 6.5 to an initial A_{600} of 0.1. The medium contained 1 mM Ca^{2+}, and free Ca^{2+} levels were controlled by adding varying amounts of EGTA. Growth was monitored by the change in A_{600} of 0.8-mL samples for 24 h.

Isolation of Yeast Membranes

Transformants were inoculated into 20 mL of SC-URA medium and incubated overnight. The culture was diluted 10-fold into SC-URA medium and grown overnight to an A_{600} of 1 to 1.8. The cells were pelleted at 4,000*g* for 5 min, washed with 10 mL of distilled water, and pelleted again. Membranes were isolated using the glass bead method (Serrano, 1988) with some modification (Liang and Sze, 1998). Cells were suspended in 10 mL of glass beads buffer (GBB) containing 10% (w/w) Suc, 25 mM 4-(2-hydroxyethyl)-1-piperazineethanesulfonic acid (HEPES)-KOH (pH 7.5), 2 mM EGTA, and 2 mM dithiothreitol, and pelleted. Typically 1- to 2-g cells were suspended in 4 to 5 mL of GBB plus 1 mM phenylmethylsulfonyl fluoride (PMSF), 0.1 mM *N*-tosyl-L-Phe chloromethyl ketone (TPCK), 10 mM benzamidine, 5 μg/mL pepstatin, and leupeptin.

Acid-washed glass beads (Sigma-Aldrich, St. Louis) were added to the meniscus, and cells were mixed on a vortex six times for 30 s each with intermittent chilling. The lysate was centrifuged at 5,000*g* for 5 min. The supernatant was layered onto a 20% and 45% (w/w) Suc step gradient containing 25 mM HEPES-KOH (pH 7.0), 1 mM dithiothreitol, 0.2 mM PMSF, and 5 mM benzamidine, and centrifuged at 108,000*g* for 3 h. Membranes at the 20%:45% (w/w) Suc interface were collected (1.3–1.5 mL) and diluted with 10 mL of 10% (w/w) Suc in 25 mM HEPES-1,3-bis (Tris[hydroxymethyl]methylamino) propane (BTP) (pH 7.0), 1 mM PMSF, 0.1 mM TPCK, 10 mM benzamidine, and 5 μg/mL pepstatin and leupeptin. After centrifugation at 108,000*g* for 1 h, the pellet was suspended in 0.5 mL of the same buffer solution and stored at −80°C. The protein concentration was determined with the Bio-Rad reagent (Bio-Rad, Hercules, CA).

Ca^{2+} Transport

$^{45}Ca^{2+}$ uptake into vesicles was measured by the filtration method (Hwang et al., 1997). All experiments were conducted with membranes isolated from two to three independent transformants. A reaction mixture (final volume 0.25 mL) contained 10 to 25 μL of vesicles (15–30 μg of protein), 200 mM Suc, 25 mM HEPES-BTP (pH 7.0), 20 mM KCl, 0.1 mM NaN_3, 100 μM EGTA, 10 μM $^{45}CaCl_2$ (1 μCi/mL), and 3 mM $MgCl_2$. Usually 1 μM bafilomycin A and 5 μM carbonyl cyanide *m*-chlorophenyl hydrazone (CCCP) were included to eliminate activity of the H^+/Ca^{2+} exchanger. Transport was usually initiated with 3 mM ATP at

room temperature (22°C) for various times. Aliquots (0.23 mL) from duplicate reactions were filtered and washed with 2 mL of cold rinse solution (250 mM Suc, 2.5 mM HEPES-BTP at pH 7.0, and 0.2 mM $CaCl_2$). $^{45}Ca^{2+}$ retained on the filter was quantitated by liquid scintillation counting. Pump activity can be determined as ATP-dependent transport that is insensitive to bafilomycin and CCCP (Liang and Sze, 1998). However, considerable $^{45}Ca^{2+}$ binds to membranes in the presence of calmodulin, so pump activity was determined as vanadate-inhibited uptake in the presence of bafilomycin and CCCP. The Na vanadate concentration used was 100 μM. The kinetic parameters were determined using either a Hanes-Woolf or a Lineweaver-Burk plot. The stock concentration of calmodulin was verified spectrophotometrically using an extinction coefficient ϵ_{278} of 1,620 M^{-1} cm^{-1} (Yazawa et al., 1990).

Peptide Synthesis and Purification

Peptides corresponding to sequences at the N terminus of ACA2 were synthesized by Research Genetics (Huntsville, AL) via Fmoc solid phase synthesis (Wellings and Atherton, 1997) on chlorotrityl resins with a peptide synthesizer (Advanced ChemTech, Louisville, KY). Peptides were purified by preparative HPLC using a gradient of 0% to 80% (v/v) acetonitrile in 0.1% (v/v) trifluoroacetic acid. All of the fractions were lyophilized and verified by MALDI-TOF using Voyager mass spectrometry. The purified peptides were obtained as a triflouroacetic acid salt. The amino acid composition of the peptide was analyzed with a fully-automated amino acid hydrolyzer/derivatizer (model 420A, ABI, Sunnyvale, CA) coupled with an on-line microbore HPLC analyzer (model 130A, ABI). The internal standard used was α-amino butyric acid. The relative purity of peptide 12-36, 20-44, and 30-54 were 93%, 90%, and 94%, respectively. Peptide stocks of 1 to 2 mM were dissolved in water or in dimethyl sulfoxide, and stored at −20 C.

Sources of Chemicals

Erythrosin B (E-7505), cyclopiazonic acid (C-1530), and bovine brain calmodulin (P-2277) were obtained from Sigma-Aldrich (St. Louis). Thapsigargin was purchased from LC Service (Woburn, MA). All other chemicals were reagent grade.

RESULTS

A Truncated ACA2 Ca^{2+}-ATPase Increased Yeast Mutant Growth on Ca^{2+}-Depleted Medium

The K616 yeast mutant defective in both a Golgi and a vacuolar Ca^{2+} pump was unable to grow on Ca $^{2+}$-depleted medium (Harper et al., 1998), although the Ca^{2+} concentration limiting growth was not determined. We tested growth rates of mutants expressing either a full-length ACA2-1 or a truncated ACA2-2 as a function of Ca^{2+} concentration. The initial free Ca^{2+} concentration in the medium was adjusted by adding varying amounts of EGTA to SC-URA medium containing 1 mM Ca^{2+}, and was estimated according to the Max-Chelator program (Bers et al., 1994). In medium containing approximately 50 μM Ca^{2+}, ACA2-1 transformants grew nearly as well as wild-type strains (Fig. 1B). However, in medium containing 0.1 to 1 μM Ca^{2+}, mutants expressing the full-length ACA2-1 grew very slowly, like control mutants transformed with vector alone (Fig. 1). Only mutants expressing the N-terminal-truncated protein (Δ2–80) showed growth rates comparable to the wild-type strain (Fig. 1). Thus, the trun-

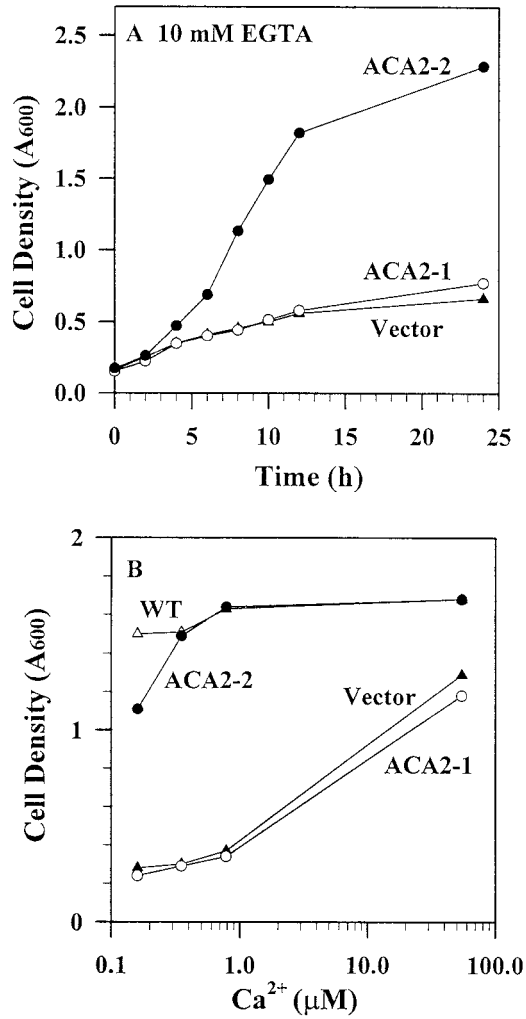

Figure 1. Expression of an N-terminal truncated ACA2 enhanced growth of yeast mutant K616 on medium containing submicromolar Ca^{2+}. A, Time-course of yeast growth on medium containing 0.16 μM Ca^{2+} and 10 mM EGTA. K616 strains were transformed with control vector alone (▲), vector containing ACA2-1 (○), and ACA2-2 (●). Transformants were suspended in SC-URA medium containing 10 mM EGTA to an initial A_{600} of 0.1. B, Submicromolar levels of extracellular Ca^{2+} support growth of wild-type yeast and transformants harboring the truncated ACA2-2. Transformants were suspended in SC-URA medium containing varying levels EGTA to give free [Ca^{2+}] ranging from 0.16 to 55 μM. Cells were then incubated for 24 h. Wild-type yeast transformed with vector control (Δ), and K616 mutant transformed with vector alone (▲), *ACA2-1* (○), or *ACA2-2* (●).

cated ACA2 protein behaved like an active Ca^{2+}-pumping ATPase on the endomembrane, while the full-length protein appeared to be inactive.

N-Terminal Truncated ACA2 Pump Is More Active Than the Full-Length Protein

To test for Ca^{2+} pump activity in vitro, yeast transformants were cultured in synthetic medium containing 1 mM Ca^{2+}, and microsomal vesicles were isolated. ATP-dependent $^{45}Ca^{2+}$ transport was measured by a filtration assay. Both a Golgi (Pmr1p) and a vacuolar (Pmc1p) Ca^{2+} pump are defective in the *K616* strain, so virtually all endogenous Ca^{2+}-pumping activity was eliminated (Liang and Sze, 1998). Most of the ATP-dependent Ca^{2+} uptake in control transformants was reduced by the protonophore CCCP and a vacuolar H^+-ATPase inhibitor, bafilomycin A (Table I), indicating that endogenous H^+/Ca^{2+} antiport activity was high. In membranes from ACA2 transformants, most (>90%) of the transport activity was due to the expressed ACA2, since the transport activity was independent of a pH gradient and sensitive to vanadate.

It was interesting that the expression of a functional ACA2 pump resulted in suppression of H^+:Ca^{2+} antiport activity in the K616 mutant, although the mechanism for this down-regulation is not known. Therefore, Ca^{2+}-pumping activity was routinely assayed with both CCCP and bafilomycin. Ca^{2+} uptake by the full-length and truncated pump was enhanced 2- and 6-fold by 10 mM K-oxalate (Table I). Although oxalate amplified the signal, it was not used in subsequent assays to better control free Ca^{2+} concentration. The expression levels of ACA2-1 and ACA2-2 in isolated yeast membranes were similar, judging by the relative immunostaining of a 110- and a 102-kD protein with a polyclonal antibody against ACA2 (Harper et al., 1998; I. Hwang, data not shown). Therefore, transport activities of the full-length and truncated ACA2 are directly comparable when expressed as nanomoles of Ca^{2+} taken up per milligram of total membrane protein. Using this analysis, the full-length pump was 10-fold less active than the truncated ACA2 (Table I) on a per milligram of protein basis when net uptake was assayed with 50 nM Ca^{2+}.

$^{45}Ca^{2+}$ uptake by ACA2 into membrane vesicles was linear for about 30 s and reached a steady state in 5 min in the absence of oxalate (Fig. 2). The transport reflects active accumulation, as most of this Ca^{2+} (>90%) was readily released by the Ca^{2+} ionophore A23187. The initial rate of Ca^{2+} pumping (>1 nmol min^{-1} mg^{-1} protein) by the truncated ACA2-2 was fast, resulting in a 4- to 10-fold higher net uptake than that of the full-length protein. The control mutants showed low uptake, probably from residual antiport activity that was not eliminated by bafilomycin and CCCP (Table I); therefore, there was little or no background pump activity in the control mutant. Because removal of the first 80 residues generated a more active pump, the results suggested that the amino-terminal region was inhibiting activity.

Calmodulin Enhanced the V_{max} of the Full-Length ACA2 Pump

Calmodulin activated Ca^{2+} pumping of the full-length ACA2 protein in a concentration-dependent fashion, with a half-maximal activation of 30 to 40 nM (Fig. 3). However, it had little or no effect on the truncated ACA2-2 pump. In the absence of calmodulin, the specific activity of the truncated ACA2 was 4- to 6-fold higher (6 nmol/mg) than that of the full-length protein (1 nmol/mg). Calmodulin stimulated ACA2-1 activity by 2- to 4-fold, suggesting a direct interaction of calmodulin with the full-length ACA2-1 protein. It is possible that calmodulin activates the pump in more than one way, because activity was sometimes further stimulated at a concentration above 0.3 μM.

In one representative experiment of four, the full-length ACA2 pump showed an apparent K_m for Ca^{2+} of 0.67 μM, and a V_{max} of 1.67 nmol mg^{-1} min^{-1} (Fig. 4). Calmodulin (0.5 μM) enhanced the maximal transport rate by 2- to 4-fold. Although the increase in affinity for Ca^{2+} was small, calmodulin consistently shifted the apparent K_m for Ca^{2+} from 0.62 to 0.43 μM (Table II). We assumed that 1 μM calmodulin does not significantly alter the free Ca^{2+} con-

Table I. *Ca^{2+} pump is detected after blocking H^+/Ca^{2+} antiport activity*

Membranes (20/45%) were isolated from yeast mutant K616 transformed with vector alone (control), *ACA2-1* (encoding full-length protein), or *ACA2-2* (encoding N-truncated protein). ATP-dependent $^{45}Ca^{2+}$ uptake at 15 min was determined in a 250-μL reaction mixture containing 250 mM Suc, 25 mM HEPES-BTP (pH 7.0), 10 mM KCl, 3 mM $MgSO_4$, 3 mM ATP, 0.2 mM NaN_3, 10 μM $CaCl_2$ (0.25 μCi/mL), and 100 μM EGTA to give a final [Ca^{2+}] of 50 nM. ΔpH-dependent activity (antiport) was estimated as the difference between Ca^{2+} uptake in the absence of any inhibitor or ionophore (total) and that in the presence of 1 μM bafilomycin A_1 and 5 μM CCCP (pump). Uptake with 10 mM K-oxalate was linear for at least 30 min.

Transformant Membrane	Ca^{2+} Uptake					
	− Oxalate			+ Oxalate		
	Total	Pump	Antiport	Total	Pump	Antiport
	nmol/mg protein at 15 min					
Control	1.32	0.07	1.25	3.41	0.10	3.31
Full-length ACA2-1	0.24	0.22	0.02	0.72	0.45	0.27
N-Truncated ACA2-2	0.99	0.88	0.11	7.00	5.93	1.07

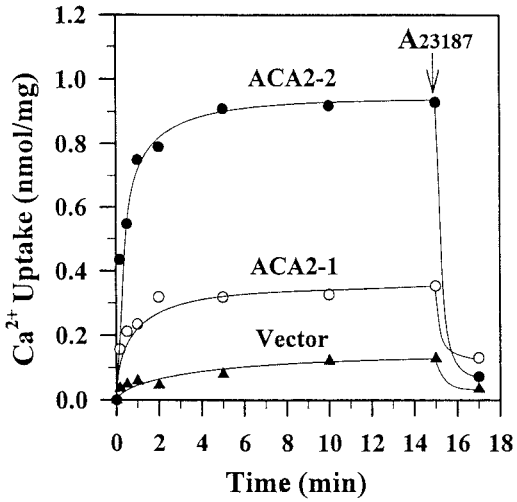

Figure 2. N-terminal-truncated ACA2 is an active Ca^{2+} pump. Membranes were isolated from mutants transformed with *ACA2-1* (○), *ACA2-2* (●), or vector alone (▲). $^{45}Ca^{2+}$ uptake into vesicles was determined in the presence of bafilomycin and CCCP with or without ATP. EGTA was used to give a free [Ca^{2+}] of 0.1 μM. Activity is expressed as ATP-dependent Ca^{2+} uptake. A23187 was added (arrow) to a final concentration of 2.5 μg/mL.

centration that is buffered with 100 μM of EGTA. Thus, the actual K_m for Ca^{2+} in the presence of calmodulin might be even lower than our minimum estimate. The truncated ACA2 showed a high affinity for Ca^{2+} (K_m = 0.25 μM) and a maximal velocity of 5 to 7 nmol mg^{-1} min^{-1} (Fig. 5; Table II). Although calmodulin stimulated the full-length pump,

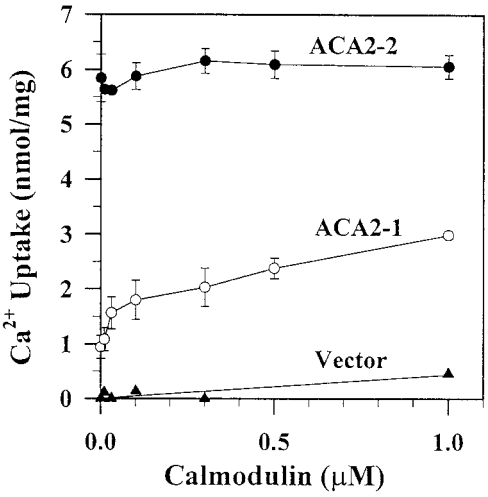

Figure 3. Calmodulin stimulated the full-length ACA2 pump but not the N-terminal truncated ACA2. Membranes were isolated from mutants transformed with *ACA2-1* (○), *ACA2-2* (●), or vector alone (▲). Net Ca^{2+} uptake (10 min) into vesicles was measured with or without 200 μM Na orthovanadate in the presence of CCCP and bafilomycin. The mixture contained 100 μM Ca^{2+} and 100 μM EGTA to give a final [Ca^{2+}] of 2.6 μM, and bovine calmodulin ranged from 0 to 1 μM. Activity is expressed as vanadate-sensitive Ca^{2+} transport. The average of two independent experiments representative of five experiments is shown.

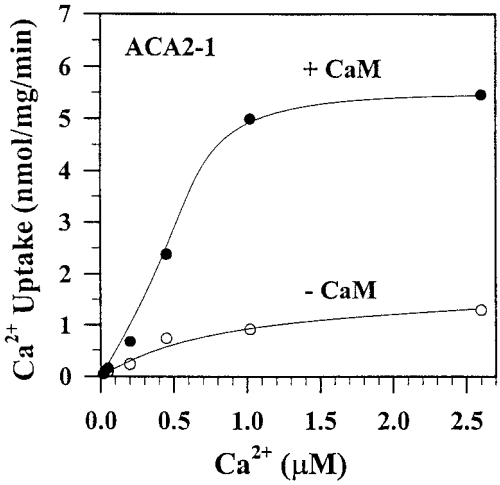

Figure 4. Calmodulin enhanced the V_{max} and the affinity for Ca^{2+} of the full-length ACA2 protein. Membranes were isolated from *ACA2-1* transformants. Initial rate of vanadate-sensitive Ca^{2+} transport was determined at 30 s with (●) or without (○) 0.5 μM calmodulin in the presence of bafilomycin and CCCP. EGTA (100 μM) was added to reaction mixtures containing 1-100 μM Ca^{2+} to give free Ca^{2+} concentrations from 1 nM to 2.6 μM. The K_m for Ca^{2+} was 0.67 or 0.39 μM without or with calmodulin, respectively. The average of duplicates from one of three similar experiments is shown.

it usually failed to stimulate it to the levels seen for the truncated protein.

Substrate Specificity

ATP is the preferred substrate of ACA2. The relative transport activity driven by 3 mM of ATP, ITP, or GTP was 1.0, 0.59, or 0.23, respectively. These results agree with previous studies showing that calmodulin-stimulated

Table II. *Effect of calmodulin or peptide 20–44 on the V_{max} and K_m for Ca^{2+} of ACA2*

The effect of 0.5 μM calmodulin on the K_m for Ca^{2+} and the V_{max} of the full-length ACA2-1 were estimated from several Lineweaver-Burk plots. Membranes were isolated from ACA2-1 transformants. EGTA (100 μM) was added to reaction mixtures containing 1 to 100 μM Ca^{2+} to give free Ca^{2+} concentrations from 1 nM to 2.6 μM. The initial rate of vanadate-sensitive Ca^{2+} transport was determined at 30 s in the presence or absence of calmodulin. The effect of peptide 20–44 on $^{45}Ca^{2+}$ pumping by the truncated ACA2-2 was determined as a function of Ca^{2+} concentration as described above. Microsomal membranes were incubated with or without 4 μM peptide 20–44 for 10 min. Transport was started with ATP and stopped at 30 s. Pump activity was determined as orthovanadate-inhibited and bafilomycin- and CCCP-resistant Ca^{2+} uptake. Averages (±SE) from three to four experiments using three separate membrane preparations are shown.

ACA Protein	Addition	K_m for Ca	V_{max}
		μM	nmol $mg^{-1}min^{-1}$
Full-length	− Calmodulin	0.62 ± 0.02	2.27 ± 0.07
ACA2-1	+ Calmodulin	0.43 ± 0.05	5.10 ± 0.26
Truncated	− Peptide 20–44	0.25 ± 0.02	7.07 ± 0.62
ACA2-2	+ Peptide 20–44	0.51 ± 0.03	3.34 ± 0.22

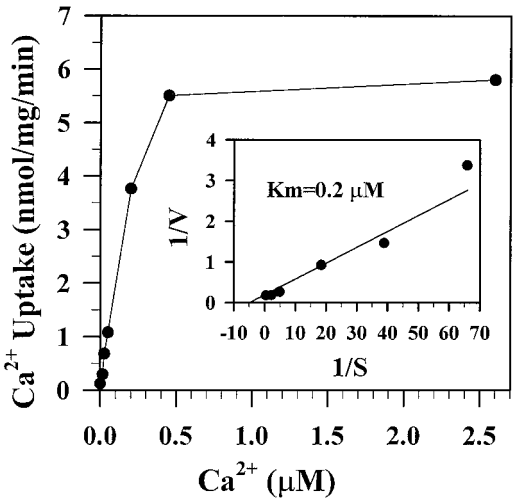

Figure 5. N-terminal truncated ACA2 pumps Ca^{2+} with high velocity and affinity. Membranes were isolated from yeast expressing ACA2-2. The initial rate of vanadate-sensitive Ca^{2+} uptake (30 s) was determined as a function of external [Ca^{2+}] in the presence of bafilomycin and CCCP. The K_m for Ca^{2+} of 0.2 μM was estimated using a Lineweaver-Burk plot. The average of duplicates from one of three experiments is shown.

Ca^{2+}-pumping ATPases from plants utilized both ITP and GTP (Rasi-Caldogno et al., 1995; Hwang et al., 1997). The ATP concentration dependence of Ca^{2+} uptake by ACA2 was complex (data not shown). The initial rate of Ca^{2+} uptake showed two apparent affinities for ATP. The K_m of the high-affinity and low-affinity sites were estimated as 120 μM and 1.2 mM, respectively. GTP-driven transport showed one apparent affinity for GTP estimated as being higher than 1.2 mM.

The ACA2 Pump Is Not Inhibited by Cyclopiazonic Acid

Orthovanadate inhibited pumping with an IC_{50} of 30 μM (Fig. 6A), which is consistent with idea that ACA2 is a phosphorylated-type ion-pumping ATPase. Erythrosin B, a potent inhibitor of both PM-type and ER-type Ca^{2+}-ATPase, completely inhibited Ca^{2+} transport activity of ACA2 at 10 μM (50% inhibition at 0.3 μM) (Fig. 6B). Thapsigargin, a specific animal sarcoplasmic/endoplasmic reticulum Ca^{2+} (SERCA) inhibitor at 4 nM, had no effect on Ca^{2+} pumping by ACA2 up to concentrations of 1,000 pmol/mg protein or 100 nM (Fig. 6C). In contrast to an Arabidopsis ER-type Ca^{2+} pump (AtECA1), cyclopiazonic acid had no effect on ACA2-catalyzed Ca^{2+}-pumping activity (Fig 6D). This inhibitor blocked the AtECA1 pump by 50% at 3 nmol/mg protein (Liang and Sze, 1998). Inhibition at high concentrations (30–100 nmol/mg protein) is thought to be non-specific, as cyclopiazonic acid com-

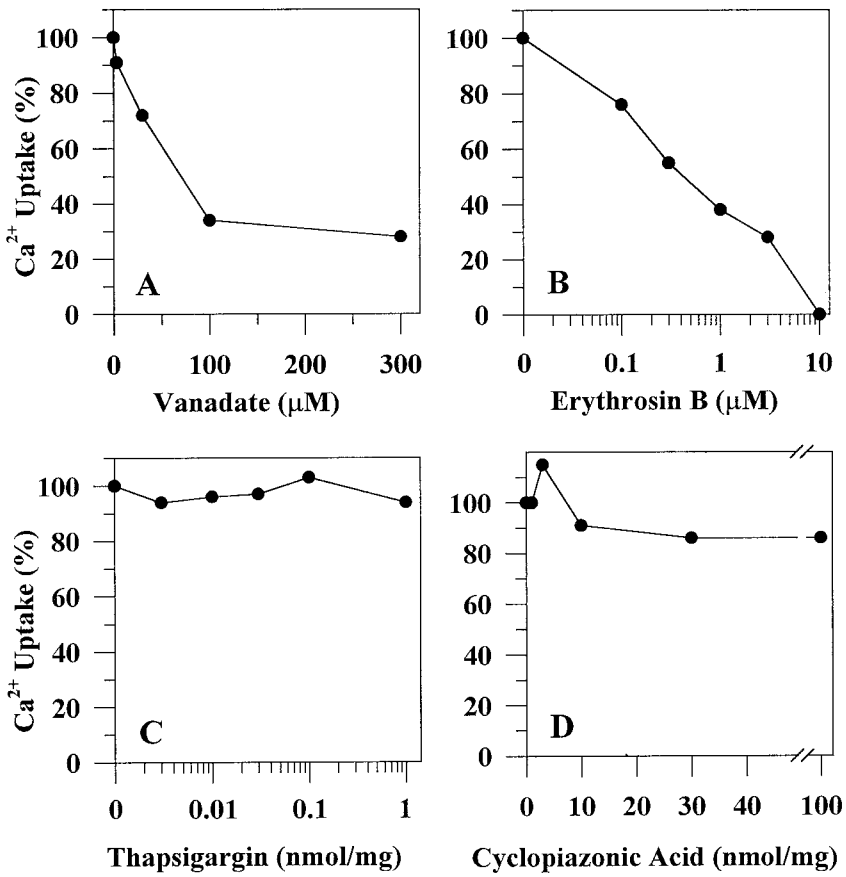

Figure 6. Sensitivity of the truncated ACA2 pump to various inhibitors: A, Orthovanadate; B, erythrosin B; C, thapsigargin; and D, cyclopiazonic acid. Vesicles isolated from ACA2-2 transformants were incubated with inhibitors for 10 min at room temperature in the reaction mixtures. Then net ATP-dependent Ca^{2+} uptake was measured in the presence of bafilomycin and CCCP. Activity (5.2 nmol mg^{-1} $protein^{-1}$) without the inhibitors used in A through C was set to 100%. To test cyclopiazonic acid in D, ATP was lowered to 0.6 mM, which gave a control activity of 1.5 nmol/mg.

pletely inhibits the SER Ca^{2+} pump at 8 nmol/mg protein at low ATP concentrations (Seidler et al., 1989). These results demonstrate that the ACA2 pump is biochemically distinct from the SER-type Ca^{2+}-ATPase consistent with their low sequence similarity (<32%) (Harper et al., 1998).

Truncated ACA2 Pump Is Inhibited by a Peptide That Consists of Residues 20 to 44

To determine the precise region responsible for inhibition, we tested whether synthetic peptides corresponding to overlapping regions in the N-terminal domain could block transport of the constitutively active truncated pump. A 25-residue peptide including Val-20 to Leu-44 inhibited Ca^{2+} transport of the truncated ACA2 by 50% at 4 μM (Fig. 7A). In contrast, another peptide that included Lys-12 to Arg-36 had no effect up to 20 μM. A third peptide corresponding to Val-30 to Arg-54 inhibited activity only by 20% inhibition at 20 μM. Since peptide 20-44 consisted of seven positively charged residues at neutral pH, we tested whether a positively charged peptide (+5) conferred inhibition. The CCa20 peptide, with 20 residues, corresponds to the region $GR^{+}CTSGAR^{+}SR^{+}SK^{+}SSLK^{+}HK^{+}AE^{-}$ at the carboxyl terminus of an ER-type Ca^{2+} pump from carrot (Liang, 1998). However, this peptide had no effect up to 10 μM (not shown). Therefore, the sequence and structure of the 20-44 peptide was sufficient to block the truncated ACA2 pump.

We tested whether 4 μM of peptide 20-44 changed the kinetic properties of the truncated pump. The affinity for Ca^{2+} was decreased by 2-fold, so that the K_m of the truncated pump increased from 0.25 to 0.51 μM Ca^{2+} (Table II). The maximal transport velocity decreased from 7.07 to 3.34 nmol mg^{-1} min^{-1}, which is consistent with the inhibition by 50% at 4 μM peptide (Fig. 7A). Thus, the peptide altered the kinetic properties of the truncated pump in a manner analogous to that imposed by the intact N-terminal domain on the full-length pump.

Peptide 20-44 Reduces Calmodulin-Stimulated Activity of the Full-Length ACA2

We tested whether peptide 20-44 inhibited the full-length pump in the presence of calmodulin. Membranes were incubated for 10 min with calmodulin in the presence of varying concentrations of peptide before Ca^{2+} pump activity was determined. Surprisingly, a peptide concentration of 0.6 μM was sufficient to block 50% of the activity stimulated by 1 μM calmodulin (Fig. 8). This peptide concentration is significantly (7-fold) lower than that (4 μM) required to block the unregulated truncated pump by 50% (Fig. 7). The results suggested that two different mechanisms were responsible for peptide inhibition of the truncated ACA2-2 versus the calmodulin-stimulated full-length ACA2-1.

Furthermore, the peptide concentration required for half-maximal inhibition of the full-length pump was dependent on the calmodulin concentration. At 0.25 μM calmodulin, 0.15 μM peptide was required to inhibit activity by 50% (Fig. 8), whereas at 1 μM calmodulin, 0.6 μM peptide blocked 50% of the activity. Thus, the peptide antagonizes the stimulation of the full-length pump by calmodulin in a concentration-dependent manner. Because calmodulin was previously shown to bind to the N-terminal region within residues 20 to 36 (Harper et al., 1998), one interpretation of these results is that peptide

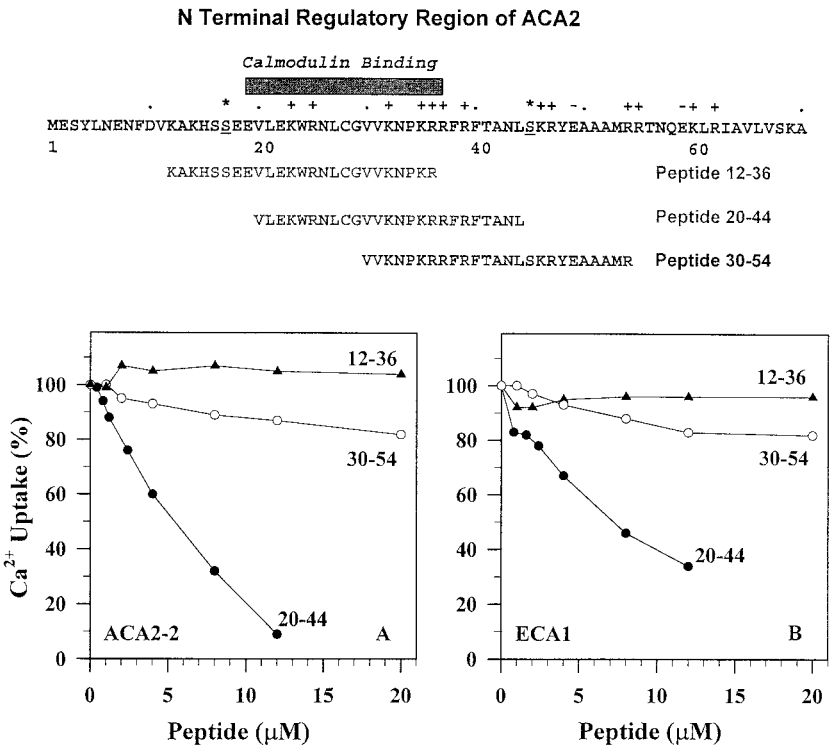

Figure 7. Peptide 20-44 inhibited Ca^{2+} pumping of the truncated ACA2 (left panel) and ECA1 (right panel). Membranes isolated from either *ACA2-2* or *ECA1* transformants were incubated with varying concentrations of peptides 12-36 (▲), 20-44 (●), or 30-54 (○). Peptides correspond to overlapping sequences between residues 12 through 54 of ACA2 shown at the top. Charged residues are marked with + or −; asterisk (*) indicates potential phosphorylation sites. Vanadate-inhibited Ca^{2+} transport (10 min) was measured at 50 nM Ca^{2+}. The results are the mean of duplicates. Activity in the absence of peptide was set to 100%, which corresponds to 1.25 and 0.89 nmol/mg for ACA2 and ECA1, respectively.

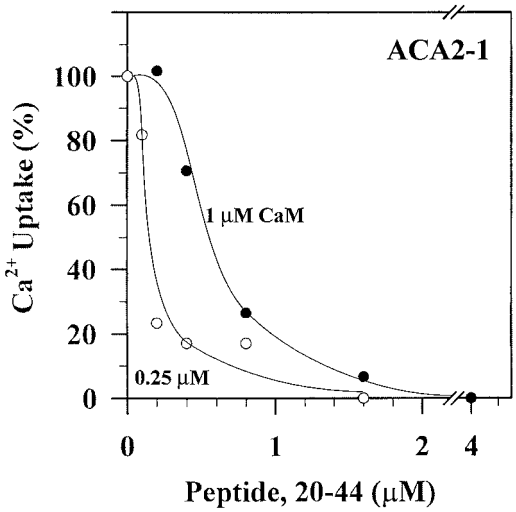

Figure 8. Peptide 20-44 antagonized the stimulation of the full-length pump by calmodulin. Membranes isolated from *ACA2-1* transformants were incubated with 0, 0.25, or 1.0 μM calmodulin alone, or with peptide 20-44 for 10 min. ATP was added to initiate transport at saturating Ca^{2+} (2.6 μM). Orthovanadate-inhibited uptake at 10 min is plotted. In the absence of peptide, the activity (100%) stimulated by 0.25 or 1.0 μM calmodulin was 2.85 or 4.0 nmol/mg, respectively. The data are from two experiments.

20-44 interacts directly with calmodulin. If this is the case, then peptide 20-44 inhibits the calmodulin-activated full-length Ca^{2+} pump indirectly according to the following model: Peptide 20-44 competes with the corresponding region in the intact N-terminal domain of the pump for calmodulin binding. When the peptide level is low, calmodulin interacts with the N-terminal region to activate the pump. With excess peptide, most of the calmodulin interacts with the peptide, leaving little or no calmodulin to activate the full-length pump. Therefore, most of the pumps remain in their autoinhibited state.

Peptide 20-44 Also Inhibits Ca^{2+} Pumping by ECA1

Peptide 20-44 was also effective in blocking transport of an ER-type Ca^{2+} pump, ECA1, from Arabidopsis (Liang et al., 1997; Liang and Sze, 1998). The concentration required for 50% inhibition was about 6 to 7 μM, and 70% of the activity was blocked by 12 μM (Fig. 7B). Therefore, 20 -44 was nearly as potent in blocking ECA1 as the ACA2 pump, suggesting that the target site of the peptide may be conserved among two distinct Ca^{2+} pumps.

DISCUSSION

An important step in understanding the regulation of intracellular Ca^{2+} in plants is to determine the kinetic properties of each Ca^{2+} transporter and the conditions that modulate its activity. Arabidopsis has at least 11 putative Ca^{2+} pumps (Geisler et al., 1999), so the distinct properties, regulation, and location of each are important in determining the pattern or form of Ca^{2+} signals within the cell. *AtECA1* encodes the first plant Ca^{2+} pump to be characterized biochemically after expression in yeast (Liang and Sze, 1998). However, it is not known how the ER-localized ECA1 pump is regulated in plants. We provide the first direct evidence, to our knowledge, that *ACA2* encodes another Ca^{2+} pump, and show that its kinetic properties are modulated by calmodulin and by an autoinhibitory sequence.

The Amino-Terminal Domain Contains an Autoinhibitor

We determined the kinetic properties of the truncated and the full-length pump, and show that in the absence of Ca^{2+}/calmodulin, the N-terminal region (between residues 2–80) functions as an autoinhibitor that decreases the V_{max} by 3-fold and the affinity for Ca^{2+} by 2.5-fold (Table II). The quantitative differences are probably underestimated, as the transport reported in Table II was conducted in the absence of oxalate. In its presence, Ca^{2+} uptake is prolonged, as Ca^{2+} in the vesicles is trapped by oxalate and back inhibition is prevented. Under these conditions, the N-terminal-truncated ACA2-2 pump was 10-fold more active than the full-length ACA2-1 protein (Table I). These results are consistent with an initial qualitative study that used ATP hydrolysis to measure the activity of a full-length and a truncated Ca^{2+}-ATPase (Harper et al., 1998). Assuming that the relative activities in vitro are comparable to those in yeast transformants, these results suggest that the basal activity of the full-length protein was not sufficient to pump enough Ca^{2+} into the ER/Golgi to support growth on Ca^{2+}-depleted medium (containing 0.1–1.0 μM Ca^{2+}).

Sequence Including Residues 20 to 44 Behaves Like the Autoinhibitory Domain

Our results indicate that a 25-residue sequence from Val-20 to Leu-44 behaved like the inhibitory region. This conclusion is supported by the following results: (a) peptide 20-44 blocked 50% activity at a concentration of 4 μM (Fig. 7A); (b) two other peptides, Lys-12-Arg-36 and Val-30-Arg-54, of similar size, charge, and partial overlapping sequence had little or no effect; and (c) peptide 20-44 at 4 μM increased the K_m for Ca^{2+} and decreased the V_{max} of the truncated pump to levels approaching the basal activity of the full-length pump (Table II). Thus, the peptide mimicked the natural inhibitor of the pump. The micromolar levels of peptide required for inhibition was similar to other chemical inhibitors, which must "find" its target site on ACA2 in a dilute membrane mixture. Our results suggest that the secondary and tertiary structures of peptide 20-44 are sufficient for inhibition.

Calmodulin Partially Activates the Full-Length Pump

In a previous study, we showed that ATP hydrolysis by the full-length protein was increased by 100 μM Ca^{2+}, and that this Ca^{2+}-ATPase activity was further stimulated by calmodulin (Harper et al., 1998). However, the affinity of ACA2 for Ca^{2+} was not known. Here we demonstrate that calmodulin stimulated the V_{max} and increased the affinity

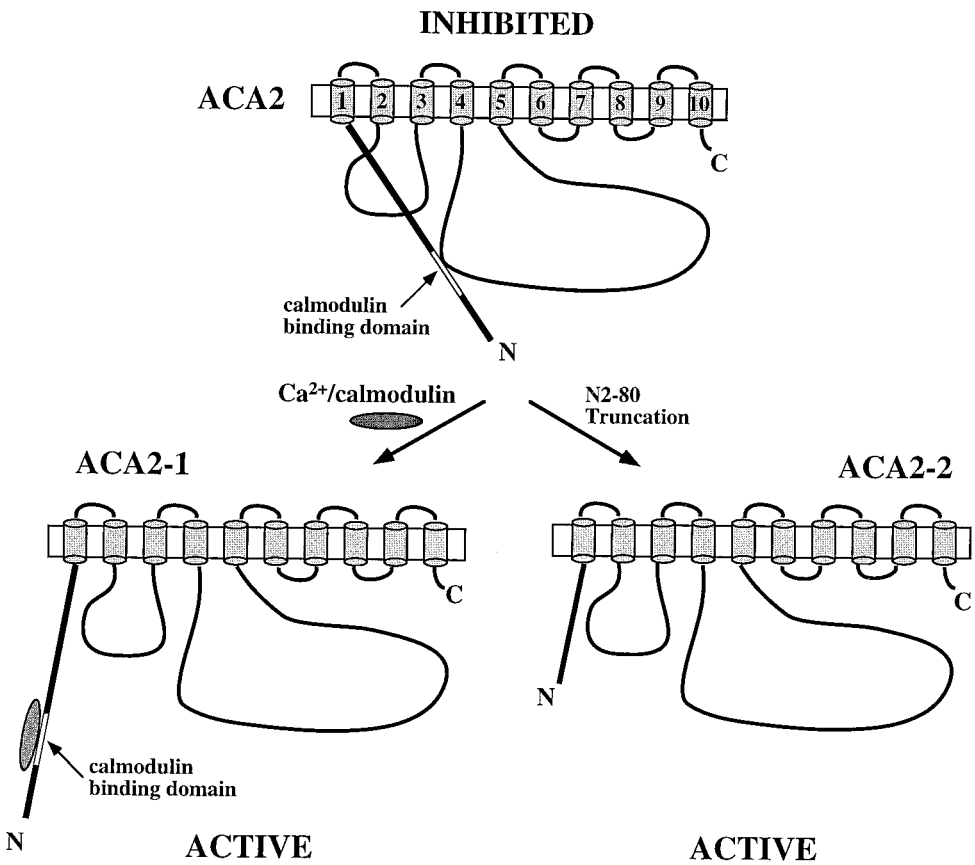

Figure 9. Working model of the regulation of ACA2 pump by an N-terminal domain. In an unstimulated cell, the full-length pump (ACA2-1) is inhibited by an intramolecular interaction of an N-terminal region with part(s) of the catalytic and hydrophilic loop(s) (top). After a stimulus, an increase in [Ca^{2+}] leads to the binding of Ca^{2+}-calmodulin complex to a region near the autoinhibitory sequence. The resulting conformational change displaces the autoinhibitory domain from its interaction with the hydrophilic loop(s), thus activating the pump (left). An N-terminal truncated pump (ΔN2-80) is therefore constitutively active and unresponsive to calmodulin (right). Numbers refer to putative transmembrane domains. N and C refer to the amino and carboxyl termini, respectively.

of the full-length ACA2-1 for Ca^{2+} (Table II). Furthermore, the affinity for Ca^{2+} of the calmodulin-stimulated full-length pump (K_m = 0.4 μM) and of the truncated pump (K_m = 0.2 μM) was about 2- and 3-fold higher, respectively, than that of the basal ACA2-1 (K_m = 0.64 μM) (Table II). Thus, ACA2 is active in the physiological range of Ca^{2+} fluctuations within the cytosol (0.1–1.0 μM). Assuming that the V_{max} of the truncated pump represents the latent potential of a full-length pump, only a partial activation of the full-length pump occurs with the addition of calmodulin. It is also possible that other modulators, such as phosphorylation or lipids, could further shift the steady-state balance between an activated and autoinhibited state.

Calmodulin Interacts with the Autoinhibitory Region

Interestingly, results from two separate approaches support the idea that the calmodulin-binding region overlaps with the inhibitory region. First, a calmodulin-binding site was identified between residues 20 and 36, as shown by the Ca^{2+}-dependent binding of calmodulin to a series of fusion proteins from the N-terminal domain (Harper et al., 1998). Second, peptide 20-44 blocked the calmodulin activation of a full-length pump (Fig. 8). This peptide inhibition was prevented by increasing the concentration of calmodulin, which is consistent with a model that the peptide competes with the pump for binding calmodulin. As the peptide concentration increases, less free calmodulin is available for interaction with the full-length pump, and thus most of the pumps remain in an inhibited conformation. The peptide at 0.2 and 0.8 μM inhibited nearly 80% of the pump activity stimulated by 0.25 and 1 μM calmodulin, respectively, supporting a model that the peptide binds calmodulin with high affinity.

Although other models are possible, the inhibition of calmodulin-stimulated ACA2 by peptide 20-44 is strikingly similar to the effect of an autoinhibitor peptide on a calmodulin-stimulated plasma membrane Ca^{2+}-ATPase from human erythrocytes (Enyedi et al., 1989; Penniston and Enyedi, 1998). The concentration of peptide C28W required for half-maximal inhibition was highly dependent on the calmodulin concentration. Furthermore, in the presence of Ca^{2+}, peptide C28W interacted tightly with calmodulin, forming a 1:1 complex. Our results support the

idea that calmodulin binds to a region overlapping the autoinhibitory domain within residues 20 to 44. The degree of overlap between the two regulatory domains has yet to be determined, since a complete calmodulin-binding domain possibly extends beyond residue 36.

Role of ACA2 and a Model for Regulation

ACA2 was recently localized to the ER of Arabidopsis roots by membrane fractionation, immunostaining, and imaging of a green fluorescent protein-tagged enzyme (Hong et al., 1999). The presence of calmodulin-stimulated Ca^{2+} pumps at the ER was regarded with skepticism for many years, because calmodulin-insensitive Ca^{2+} pumps such as AtECA1 are commonly associated with the ER (Liang et al., 1997). However, biochemical studies using a variety of plant tissues had initially suggested that ER was another site for calmodulin-stimulated Ca^{2+} pumps (Hwang et al., 1997, and refs. therein). Although it is unclear what roles two differentially regulated Ca^{2+} pumps play at the ER (Hong et al., 1999), the results support the idea for discrete functional domains (Staehelin, 1997) and for spatially and functionally distinct Ca^{2+} stores (Golovina and Blaustein, 1997) in the ER. Signals that stimulate ER functions, including protein assembly, modification, and vesicle trafficking, could conceivably modulate ER-localized Ca^{2+} pumps. For instance, GA_3-stimulated a 2-fold increase in calmodulin and Ca^{2+} uptake in the ER of barley aleurone cells, suggesting that elevated calmodulin and Ca^{2+} in the ER may regulate Ca^{2+}-dependent α-amylase synthesis in the lumen of the ER (Gilroy and Jones, 1993).

We propose a working model for the regulation of the ACA2 pump (Fig. 9). In a resting cell, ACA2 is less active due to an interaction of the N-terminal autoinhibitory region including residues 20 to 44 with an intramolecular hydrophilic region. After a signal induces an increase in calmodulin or in cytosolic Ca^{2+} near ACA2 (or both), the Ca^{2+}-calmodulin complex binds to a region including residues 20 to 36. This binding confers a conformational change to the N-terminal domain, resulting in the dissociation of the inhibitory region from the hydrophilic loop(s) leading to an activated state. The N-terminal truncated protein is therefore constitutively active as the inhibitory domain is absent. However, it can be inactivated by a synthetic peptide with a sequence (residues Val-20 to Leu-44) corresponding to the inhibitory domain.

It is unclear what part(s) of the pump interacts with the autoinhibitory sequence within residues 20 to 44 at the N-terminal domain. The structural elements that interact with the peptide may be common in two distinct types of Ca^{2+} pumps, as peptide 20-44 also blocked Ca^{2+} pumping of AtECA1 (Fig. 7B). Interestingly, a synthetic peptide having the sequence of the autoinhibitory domain of the animal plasma membrane Ca^{2+}-ATPase also inhibits SERCA activity (Enyedi and Penniston, 1993). Several highly conserved regions common to P-type ATPases include the region surrounding the aspartyl phosphorylation site and that involved in ATP binding between transmembrane regions 4 and 5. One working model is that the N-terminal autoinhibitory domain interacts with sites located within or near two cytoplasmic loops located between TM4 and TM5 and between TM2 and TM3. In cross-linking studies, the peptide from the C-terminal domain of plasma membrane Ca^{2+}-ATPase appears to interact with a region between the acyl phosphorylation site and the ATP-binding site (Falchetto et al., 1991). Thus, in spite of an amino-terminal location in ACA2, the regulatory domains in both animal and plant pumps appear to have evolved with a common mechanism of regulation (James et al., 1995).

The regulation of ACA2 bears striking similarities to a 133-kD plasma membrane Ca^{2+} pump (Rasi-Caldogno et al., 1995) and a 111-kD vacuolar Ca^{2+} pump (Askerlund, 1996). In both cases, trypsin treatment of membrane vesicles resulted in a 2- to 3-fold activation of Ca^{2+} pumping and loss of calmodulin sensitivity. The activation by trypsin was accompanied by a decrease of the intact vacuolar Ca^{2+} pump of 111 kD, and the appearance of a 102-kD polypeptide. However, only the 111-kD protein bound calmodulin, suggesting that trypsin had removed the calmodulin-binding region. The location of the calmodulin-binding region was unclear until the corresponding gene, *BCA1*, was cloned. Calmodulin was shown to bind with high affinity (K_D = 75 nM) to a peptide corresponding to Ala-19-Leu-43 (Malmstrom et al., 1997). Thus, a vacuolar BCA1, an ER-localized ACA2, and possibly a plasma membrane Ca^{2+} pump (M.I. de Michelis, personal communication) are all regulated by an N-terminal domain similar to the model of Figure 9. Additional homologs of ACA2 and BCA1 are being identified in Arabidopsis (for review, see Geisler et al., 1999), so a future challenge is to understand the distinct cellular and physiological roles of each Ca^{2+} pump in plants.

ACKNOWLEDGMENTS

We thank Rajini Rao (Johns Hopkins University, Baltimore) and John Penniston (Mayo Clinic, St. Paul) for stimulating and enlightening discussions.

Received July 26, 1999; accepted September 10, 1999.

LITERATURE CITED

Askerlund P (1996) Modulation of an intracellular calmodulin-stimulated Ca^{2+}-pumping ATPase in cauliflower by trypsin. Plant Physiol **110:** 913–922

Askerlund P (1997) Calmodulin-stimulated Ca^{2+}-ATPases in the vacuolar and plasma membranes in cauliflower. Plant Physiol **114:** 999–1007

Becker DM, Guarente L (1991) High-efficiency transformation of yeast by electroporation. Methods Enzymol **194:** 186–187

Bers D, Patton C, Nuccitelli R (1994) A practical guide to the preparation of Ca^{2+} buffers. *In* Methods in Cell Biology, Vol 40: A Practical Guide to the Study of Ca^{2+} in Living Cells. Academic Press, New York

Bonza C, Carnelli A, De Michelis MI, Rasi-Caldogno F (1998) Purification of the plasma membrane Ca-ATPase from radish seedlings by calmodulin-agarose affinity chromatography. Plant Physiol **116:** 845–851

Bush DS (1995) Calcium regulation in plant cells and its role in signaling. Annu Rev Plant Physiol Plant Mol Biol **46:** 95–122

Cunningham KW, Fink GR (1994) Calcineurin-dependent growth control in *Saccharomyces cerevisiae* mutants lacking PMC1, a homolog of plasma membrane Ca^{2+} ATPases. J Cell Biol **124:** 351–363

Enyedi A, Penniston JT (1993) Autoinhibitory domains of various Ca transporters cross react. J Biol Chem **268:** 17120–17125

Enyedi A, Vorherr T, James P, McCormick DJ, Filoteo AG, Carafoli E, Penniston JT (1989) The calmodulin binding domain of the plasma membrane Ca pump interacts both with calmodulin and with another part of the pump. J Biol Chem **264:** 12313–12321

Falchetto R, Vorherr T, Brunner J, Carafoli E (1991) The plasma membrane Ca^{2+} pump contains a site that interacts with its calmodulin-binding domain. J Biol Chem **266:** 2930–2936

Geisler M, Axelson K, Harper JF, Palmgren MG (1999) Molecular aspects of higher plant P-type Ca-ATPases. Biochim Biophys Acta (in press)

Gilroy S, Jones RL (1993) Calcium stimulation of unidirectional calcium uptake by the endoplasmic reticulum of barley aleurone. Planta **190:** 289–296

Golovina VA, Blaustein MP (1997) Spatially and functionally distinct Ca^{2+} stores in sarcoplasmic and endoplasmic reticulum. Science **275:** 1643–1648

Harper JF, Hong B, Hwang I, Guo HQ, Stoddard R, Huang JF, Palmgren MG, Sze H (1998) A novel calmodulin-regulated Ca^{2+}-ATPase (ACA2) from Arabidopsis with an N-terminal autoinhibitory domain. J Biol Chem **273:** 1099–1106

Hong B, Ichida A, Wang Y, Gens JS, Pickard BG, Harper JF (1999) Identification of a calmodulin-regulated Ca-ATPase in the ER. Plant Physiol **119**: 1165–1175

Huang L, Berkelman T, Franklin AE, Hoffman NE (1993) Characterization of a gene encoding a Ca^{2+}-ATPase-like protein in the plastid envelope. Proc Natl Acad Sci USA **90:** 10066–10070

Hwang I, Ratterman DM, Sze H (1997) Distinction between endoplasmic reticulum-type and plasma membrane-type Ca^{2+} pumps. Plant Physiol **113:** 535–548

James P, Vorherr T, Carafoli E (1995) Calmodulin-binding domains: just two faced or multi-faceted? Trends Biochem Sci **20:** 38–42

Liang F (1998) Functional identification and biochemical characterization of ER-type Ca pumps in *Arabidopsis thaliana*. PhD thesis. University of Maryland, College Park

Liang F, Cunningham KW, Harper JF, Sze H (1997) ECA1 complements yeast mutants defective in Ca^{2+} pumps and encodes an endoplasmic reticulum-type Ca^{2+}-ATPase in *Arabidopsis thaliana*. Proc Natl Acad Sci USA **94:** 8579–9584

Liang F, Sze H (1998) A high affinity Ca pump (ECA1) from the endoplasmic reticulum is inhibited by cyclopiazonic acid but not by thapsigargin. Plant Physiol **118:** 817–825

Malmstrom S, Askerlund P, Palmgren MG (1997) A calmodulin-stimulated Ca^{2+}-ATPase from plant vacuolar membranes with a putative regulatory domain at its N-terminus. FEBS Lett **400:** 324–328

Penniston JT, Enyedi A (1998) Modulation of the plasma membrane Ca^{2+} pump. J Membr Biol **165:** 101–109

Rasi-Caldogno F, Carnelli A, De Michelis MI (1992) Plasma membrane Ca^{2+}-ATPase of radish seedlings: II. Regulation by calmodulin. Plant Physiol **98:** 1202–1206

Rasi-Caldogno F, Carnelli A, De Michelis MI (1995) Identification of the plasma membrane Ca^{2+}-ATPase and of its autoinhibitory domain. Plant Physiol **108**: 105–113

Rose MD, Winston F, Hieter P (1990) Methods in Yeast Genetics: A Laboratory Course Manual. Cold Spring Harbor Laboratory Press, Cold Spring Harbor, NY

Sanders D, Brownlee C, Harper JF (1999) Communicating with calcium. Plant Cell **11:** 691–706

Seidler NW, Jona I, Vegh M, Martonosi A (1989) Cyclopiazonic acid is a specific inhibitor of the Ca^{2+}-ATPase of sarcoplasmic reticulum. J Biol Chem **264:** 17816–17823

Serrano R (1988) H^{+}-ATPase from plasma membranes of *Saccharomyces cerevisiae* and *Avena sativa* roots: purification and reconstitution. Methods Enzymol **157:** 533–544

Staehelin LA (1997) The plant ER: a dynamic organelle composed of a large number of discrete functional domains. Plant J **11:** 1151–1165

Ward JM, Pei Z, Schroeder JI (1995) Roles of ion channels in initiation of signal transduction in higher plants. Plant Cell **7:** 833–844

Wellings DA, Atherton E (1997) Standard Fmoc protocols. Methods Enzymol **289:** 44–67

Yazawa M, Matsuzawa F, Yagi K (1990) Interdomain interaction and the structural flexibility of calmodulin in the connecting region of the terminal domains. J Biochem (Tokyo) **107:** 287–291